Supporting Information Appendix

"Behavioral responses across a mosaic of ecosystem states restructure a sea otter–urchin trophic cascade"

Joshua G. Smith[1*], Joseph Tomoleoni[2], Michelle Staedler[3], Sophia Lyon[2]; Jessica Fujii[3], M. Tim Tinker[1, 2]

1. *Department of Ecology and Evolutionary Biology, University of California Santa Cruz, 115 McAllister Way, Santa Cruz CA, 95060, USA*
2. *U. S. Geological Survey, Western Ecological Research Center, Santa Cruz Field Station, 2885 Mission St., Santa Cruz CA, USA*
3. *Monterey Bay Aquarium, 886 Cannery Row, Monterey CA, 93940, USA*

*Corresponding author: JogSmith@ucsc.edu

Supporting Information Appendix. Supplementary Methods

Time-series analysis of factors leading to the formation of the mosaic. We used a multivariate correlation analysis to determine the sign (positive or negative) and strength (slope) of the relationship between *Pycnopodia* density, density of exposed purple sea urchins, kelp density, and sea otter abundance in Monterey Bay, California. The analysis revealed an inverse relationship between *Pycnopodia* density and exposed purple sea urchin density ($P < 0.0001$, $ß = -0.28$), a positive relationship between *Pycnopodia* and kelp density ($P < 0.0001$, $ß = 0.13$), and a strongly positive relationship between exposed purple sea urchins and sea otter abundance ($P < 0.0001$, $ß = 0.73$). We then used a cross-correlation analysis to determine whether a time-lag occurred between the initiation of these events, but found that the model was centered at zero, indicating that these events likely began at or around the year 2014. Although these events likely initiated simultaneously, the otter, kelp, and urchin response continued for at least three years.

Emergence of urchins following the demise of *Pycnopodia.* The exponential increase in the density of exposed purple sea urchins is explained almost entirely by the emergence of urchins from refuge in crevices that then made them detectible by divers. This behavioral response is evidenced by the dramatic increase in numbers across the entire size distribution of urchins. Counts (i.e., density) of 3 cm (approx. two years old) to 8 cm (several years old) urchins uniformly increased over a magnitude of 600% between 2013 and 2014. These size classes are too large to have settled from the plankton later than 2013, and the increase occurred across all of the survey sites, negating immigration into the survey area. However, a recruitment event may have occurred post-emergence (after 2014) that further led to the observed exponential increase in sea urchin counts.

State space model for estimating population trends. The annual census counts of independent otters and dependent pups, collected between 1990 and 2018 (1), provide a time-series of relative abundance indices for each area of the coast. Because the sea otter census is conducted as an exhaustive, un-corrected count with no associated measurement of uncertainty, the annual counts cannot be interpreted as a true estimate of abundance (2). In previous analyses of sea otter population trends, maximum likelihood or Bayesian approaches have been used to infer the underlying population dynamics while accounting for observer error (3-4). Here we describe a Bayesian state-space model used to infer trends in southern sea otter abundance within each of three coastal regions: Santa Cruz, Monterey, and Big Sur (see Figure S10). Our model explicitly incorporates demographic processes and allows for both observer error (measurement uncertainty) in the raw counts of independents and pups, as well as stochasticity (variation across years) in underlying vital rates. By utilizing an age-structured, demographically explicit process model, we can estimate realistic levels of variation in the underlying trends and ensure that the inferred dynamics are constrained to demographically feasible limits. We also gain insights into the nature of variation in underlying vital rates.

Process model

We use a simplified, female-only demographic model, whose structure and parameter value ranges are informed by previously published demographic models for southern sea otters (3-7). We define 4 age classes of independent otters: 3 subadult year classes (6mo – 1.5yr, 1.5 – 2.5yr, and 2.5-3.5yr) and a 4th multi-year class for adults that spans all ages >3.5yr. Independent otter age classes begin at 6 months because that is the average age at which dependent pups are weaned by females (8), and dependent pups are not tracked as a separate class but rather incorporated into the adult reproductive term (3) as described below. While reproduction is continuous and only weakly seasonal in southern sea otters (9), we discretize reproductive processes for model tractability such that adult females are assumed to become pregnant at the beginning of an annual time step, give birth halfway through the year, and then wean the pup (if it survives) at the end of the time step, at which time the 6mo pup recruits to the first subadult year class.

Stage-specific survival rates are described using an instantaneous hazards approach: for adults (stage 4), the annual *per-capita* survival rate is estimated as:

$$S_a = \exp\left(-\exp\left(-h_0 + \alpha\right)\right) \tag{0.1}$$

where h_0 is a constant representing baseline log-hazards (set to -3 to correspond to maximum survival of 0.95, based on previous studies (6)); and α is the mean log-hazard ratio for adults, estimated by fitting the model to survey data. For simplicity and model tractability we assume that stochasticity primarily affects subadult survival and has minimal effects on adult survival. We thus calculate sub-adult survival rates as:

$$S_{sa,t} = \exp\left(-\exp\left(h_0 + \gamma + \varepsilon_{\gamma,t}\right)\right), \quad \varepsilon_{\gamma,t} \sim normal\left(0, \sigma_\gamma\right) \tag{0.2}$$

where γ is the mean log-hazard ratio for subadults and $\varepsilon_{\gamma,t}$ is a normally distributed random parameter representing the effects of environmental stochasticity in year t, and has a mean of 0 and standard error of σ_γ (a parameter to be estimated). The survival of pups from birth to weaning is also assumed to be affected by environmental stochasticity, with annual deviations from the mean value assumed to be partially correlated and partially independent of subadult survival:

$$S_{p,t} = \exp\left(-\exp\left(h_0 + \phi + \varepsilon_{\gamma,t} + \varepsilon_{\phi,y}\right)\right), \quad \varepsilon_{\phi,t} \sim normal\left(0, \sigma_\phi\right) \tag{0.3}$$

where ϕ is an estimated parameter (representing the mean log-hazard ratio for dependent pups) and $\varepsilon_{\phi,t}$ is a normally distributed random effects term representing environmental stochasticity in year t, with mean of 0 and standard error σ_ϕ, (a parameter to be estimated).

The annual *per-capita* reproductive contributions of adult females to the first female subadult year class in year t are calculated as:

$$R_t = S_a \times \left(br/2\right) \times S_{p,t} \tag{0.4}$$

where *br* is the annual birth rate, which we held fixed at 1 (10). Equation 1.4 also assumes a 50:50 sex ratio of pups, and that pup survival to weaning is conditional upon the survival of its mother (S_a). Combining these vital rates, we calculate the annual change in abundance (n) of each of the 4 age-classes in the population through the following 4 recursive equations:

$$\begin{aligned} n_{1,t} &= n_{4,t-1} \times R_t \\ n_{2,t} &= n_{1,t-1} \times S_{sa,t-1} \\ n_{3,t} &= n_{2,t-1} \times S_{sa,t-1} \\ n_{4,t} &= \left(n_{3,t-1} \times S_{sa,t-1}\right) + \left(n_{4,t-1} \times S_a\right) \end{aligned} \tag{0.5}$$

The total expected number of independent otters in year t, $N_{\text{exp,t}}$, is calculated as the sum of the individuals in each of the 4 age classes,

$$N_{\text{exp},t} = \sum_{i=1}^{4} n_{i,t} \tag{0.6}$$

To calculate the expected number of pups that could be counted in a survey, we need to account for several complications. First, not all the pups born in a year are available to be counted at the time of the spring survey, as some will have already been weaned or died, and others will not yet have been born. We define the parameter ρ as the proportion of pups produced in year t that were born within the 6-mo. period immediately before the survey. Of those pups, a certain proportion will die before weaning (described by $1\text{-}S_{p,t}$); however, not all of those deaths will have occurred by the time of the survey, as most pups counted in spring surveys are 2mo. or younger. Incorporating both these adjustments we calculate the expected number of pups as:

$$P_{\text{exp},t} = n_{4,t}\left[\rho \times \left(br/2\right) \times \left(S_{p,t}\right)^{1/3}\right] \tag{0.7}$$

Finally, we assessed the hypothesis that there was a substantial change in mean survival rates over the study period, potentially associated with the surge in prey abundance described in this study. To evaluate this possibility we expanded the model to estimate two sets of age-specific log hazard rates, [α_1, γ_1 , ϕ_1] and [α_2, γ_2, ϕ_2], with each set corresponding to a different partition of years within the study period. While our *a priori* expectation was that a change in survival rates likely occurred sometime around 2014, we did not enforce a particular temporal break, but rather allowed this to be data driven. Specifically, we defined a vector sw_y having length Y (the number of years of the study) and with integer values of 1 or 2. For years where sw_y= 1, we apply the first set of age-specific hazard rates, while for years where sw_y= 2 we apply the second set of age-specific hazard rates. We evaluated multiple configurations of the sw_y vector corresponding to different temporal sequences of hazard rates: we allowed for up to 2 temporal breaks in demographic conditions (i.e., the possibility of a change from a series of 1's to a series of 2's, and the possibility of a later change from a series of 2's back to a series of 1's) and also evaluated a "null model" where all years experienced the same set of hazard rates. For each model configuration we compute the differences in log hazard rates between the two sets of demographic conditions:

$$\begin{aligned} \delta_\alpha &= \alpha_2 - \alpha_1 \\ \delta_\gamma &= \gamma_2 - \gamma_1 \\ \delta_\phi &= \phi_2 - \phi_1 \end{aligned} \tag{0.8}$$

These log differences are informative because the proportional change in age-specific instantaneous hazard rates from one time period to another can be calculated as exp(δ).

Data fitting

We compared the observed survey counts of independents ($N_{obs,t}$) and pups ($P_{obs,t}$) to the expected values $N_{exp,t}$ and $P_{exp,t}$ generated by the process model, using Markov Chain Monte Carlo (MCMC) methods to find the parameter values most likely to have produced the observed data. Previous analyses of sea otter surveys have found that counts are over-dispersed relative to a Poisson distribution (10), and thus can be described using negative binomial distributions:

$$N_{obs,t} \sim negative\_binomial\left(mean = N_{\exp,t}, \tau_N\right) \tag{0.9}$$

$$P_{obs,t} \sim negative\_binomial\left(mean = P_{\exp,t}, \tau_P\right) \tag{0.10}$$

where τ_N and τ_P are inverse-dispersion (or precision) parameters estimated during model fitting. We set weak priors for all parameters, including half-Cauchy priors (*cauchy*(0,1)) for standard error (σ) and prevision parameters (τ), half-normal priors (*normal*(0,1)) for α, γ and ϕ parameters, and a beta prior (*beta*(1,1)) for ρ. For each model fit we ran 20 independent chains, saving a total of 10,000 posterior samples after a burn-in of 1000 samples.

We used R (R.Core.Team 2014) and STAN (11) software to code and fit the state space model. We evaluated model convergence by graphical examination of traceplots and by ensuring the R-hat statistic was less than 1.05 for all parameters (12). We evaluated model goodness of fit via graphical posterior predictive checks (Figure S4), whereby the distributions of out-of-sample predictions generated by the model were compared with observed data (13). To determine the best-supported number and timing of temporal breaks in demographic conditions (switches between alternative sets of hazard rates), we fit models with many alternative configurations of the sw_y vector. For each fit, we calculated the posterior distributions of the log-likelihoods of observed data, which we used to compute the "Leave-out-one Information Criteria", or LooIC (14). We evaluated LooIC diagnostics to ensure goodness of fit (all Pareto k estimates < 0.5) and selected the model with the lowest LooIC value as the best-supported temporal sequence of vital rates for that region. We report tabular summaries of the posterior distributions of parameters from the best-supported model for the Monterey region (Table S1), and we present density plots of the mean and 90% credible interval (CI) of δ_α, δ_γ, and δ_ϕ for all 3 regions (Figure S5). We use the model estimated values of $N_{exp,t}$ and $P_{exp,t}$ to plot trends in abundance of pups and independent sea otters over the study period in Monterey (Figure S3) and for comparing trends in total abundance between Santa Cruz, Monterey and Big Sur (Figure S4, S5).

Supporting Information Appendix. Supplementary Tables

Table S1. Summary of parameter estimates from a Bayesian state space demographic model fit to survey data from the Monterey study area (see SI methods for parameter definitions and dynamics). The posterior distributions of each parameter are described by the mean, standard deviation, 2.5% and 97.5% quantiles (which bound the 95% CI), the effective sample size (n_eff) and the R-hat statistic, which should be close to 1 if the model converged appropriately resulting in well-mixed chains.

Parameter	mean	sd	2.50%	97.50%	n_eff	R-hat
s_g	0.3656	0.1613	0.1215	0.7429	734.6	1.022
s_f	0.3835	0.224	0.1125	0.9351	426.2	1.043
t_N	149.6	85.89	54.66	350.7	6026	1.001
t_P	41.94	188.9	9.374	167.8	4813	1.001
r	0.6913	0.0429	0.6125	0.7826	1536	1.008
a_1	0.9319	0.2666	0.2915	1.303	2511	1.008
a_2	0.2213	0.1714	0.0076	0.6272	9149	0.999
g_1	1.569	0.2519	1.142	2.093	4619	1.003
g_2	0.5824	0.296	0.1097	1.244	8245	1.001
f_1	2.145	0.387	1.494	2.977	2121	1.009
f_2	1.071	0.4379	0.3311	2.019	8525	1.001
d_a	-0.7105	0.3204	-1.209	0.02943	3411	1.005
d_g	-0.9863	0.3974	-1.722	-0.1645	5993	1.002
d_f	-1.074	0.5825	-2.165	0.1258	2976	1.005

Supporting Information Appendix. Supplementary Figures S1-S12

Figure S1. Subtidal rocky reef survey sites along the Monterey Peninsula, California, USA.

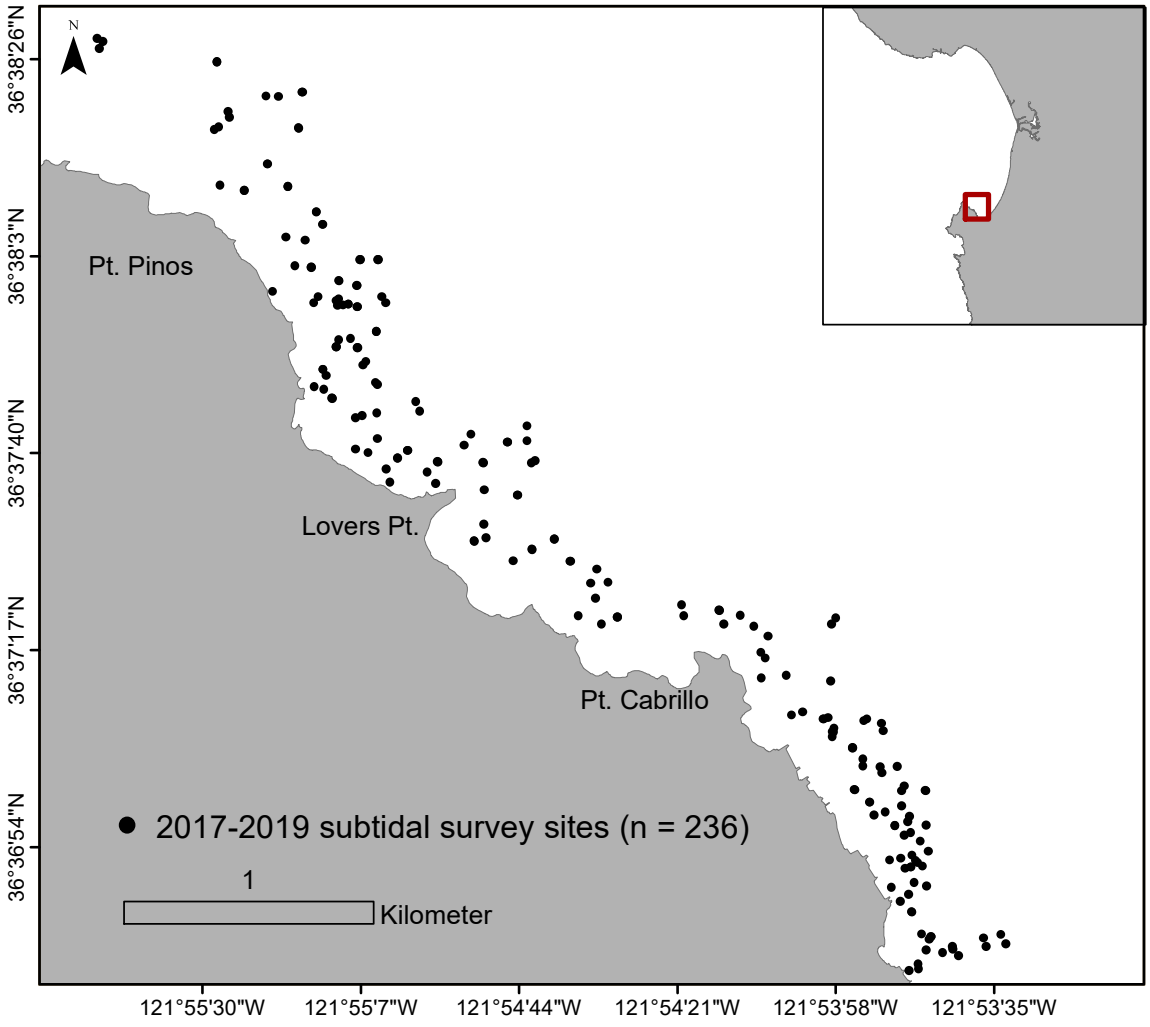

Figure S2. Subtidal survey sites (panel A) from 2018 showing the relationship between kelp density (panel B), urchin density (panel C), and gonad index (panel D). Black triangles show sea otter-sea urchin focal patches. The data in panels B-D were interpolated from 121 randomly sampled subtidal locations (both 'reference' and 'urchin focal patch' sites were sampled using the same protocol) using inverse distance weighting in ArcGIS. All interpolated maps are constrained to rocky reef in the 5–20 meters depth range.

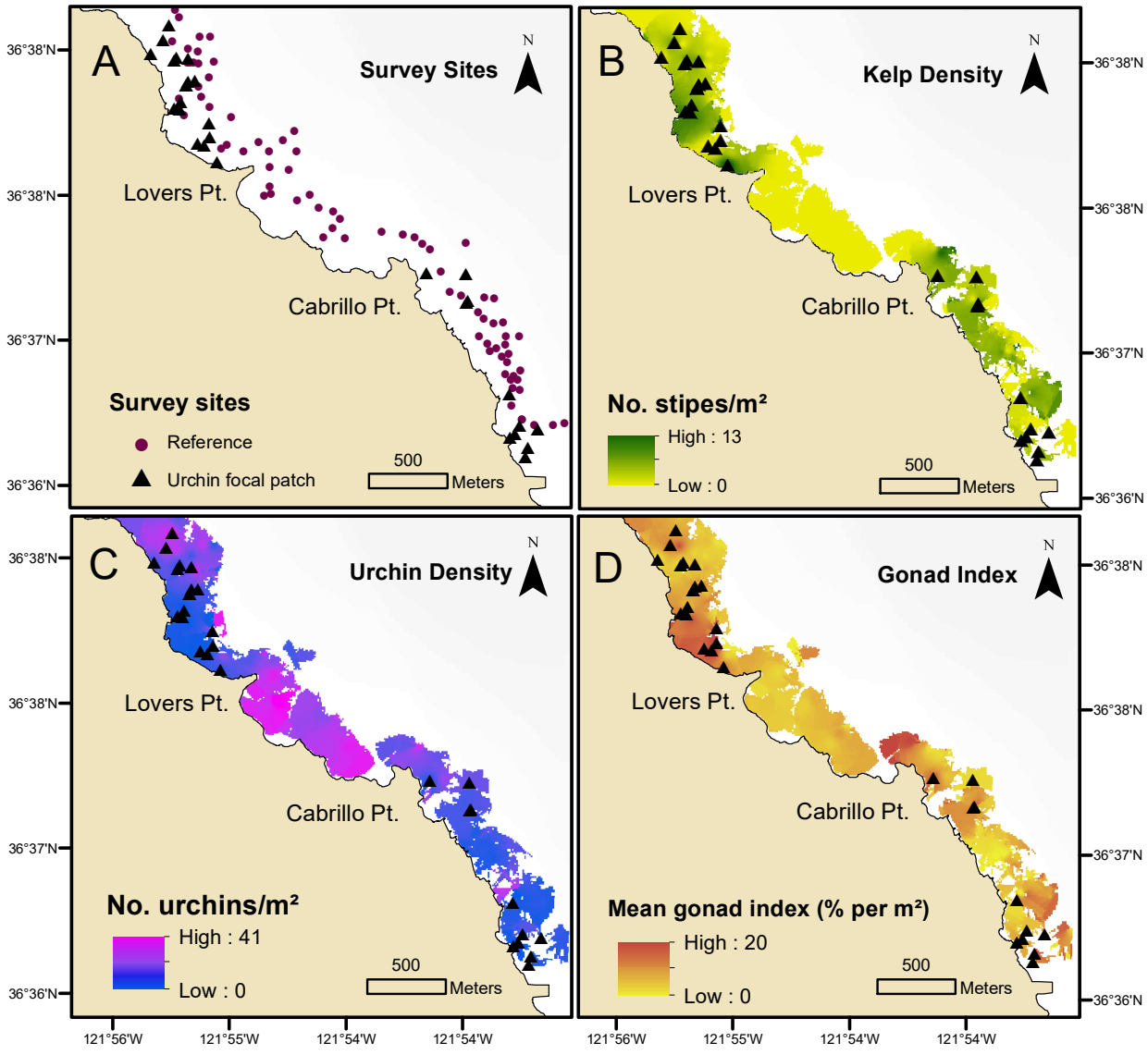

Figure S3. Trends in abundance of independent otters (blue line) and an index of pup production (orange line) for the Monterey study area, as estimated by a Bayesian state space model. The shaded band represent the 95% credible intervals (CI) around the mean estimated values.

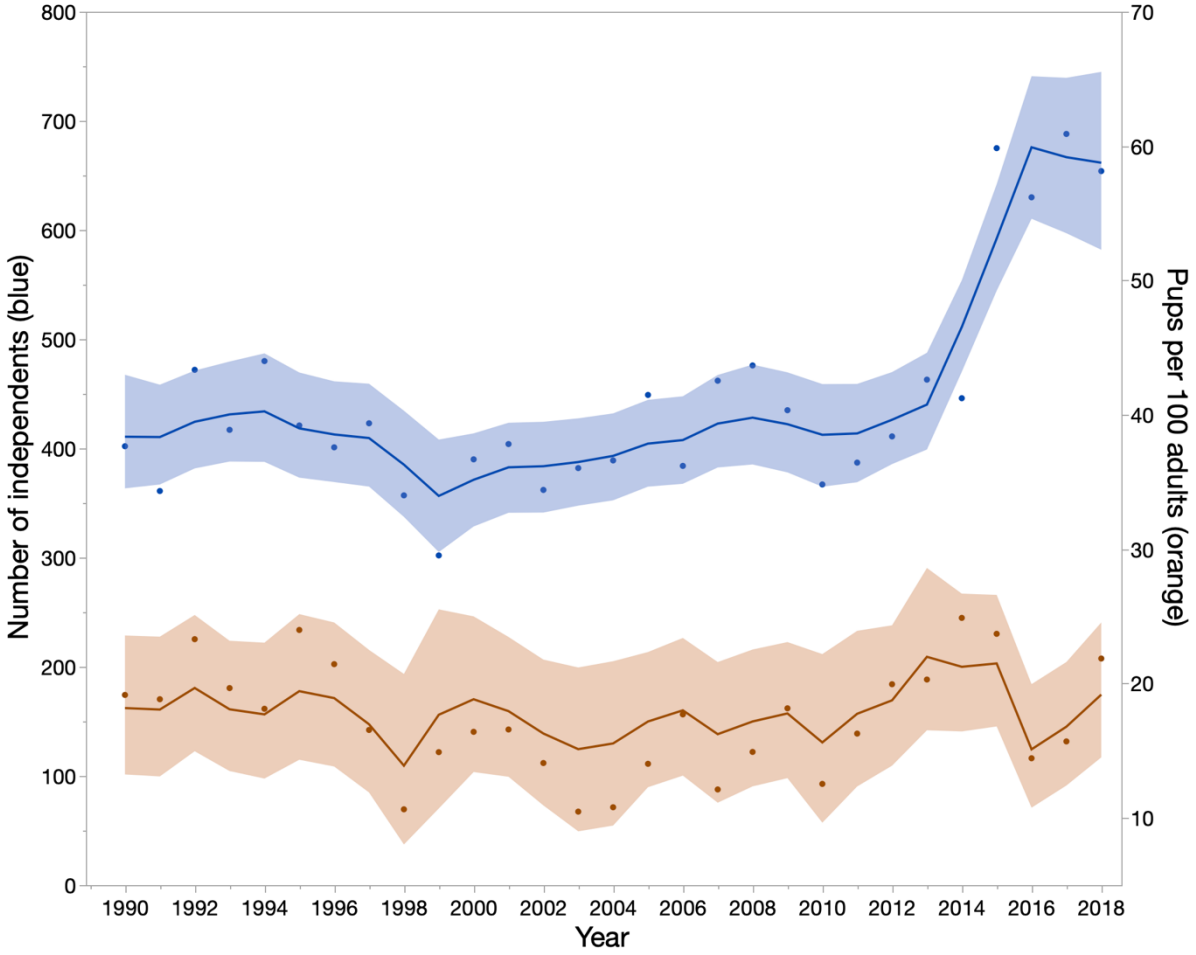

Figure S4. Posterior distributions for δ parameters estimated by a state space model fit to sea otter survey data from Santa Cruz (panel A), Monterey (panel B) and Big Sur (panel C). Each δ value represents the difference between log hazard rates for different time periods (indicated in the plot titles), and are calculated separately for adults (α), subadults (γ) and pups (ϕ).

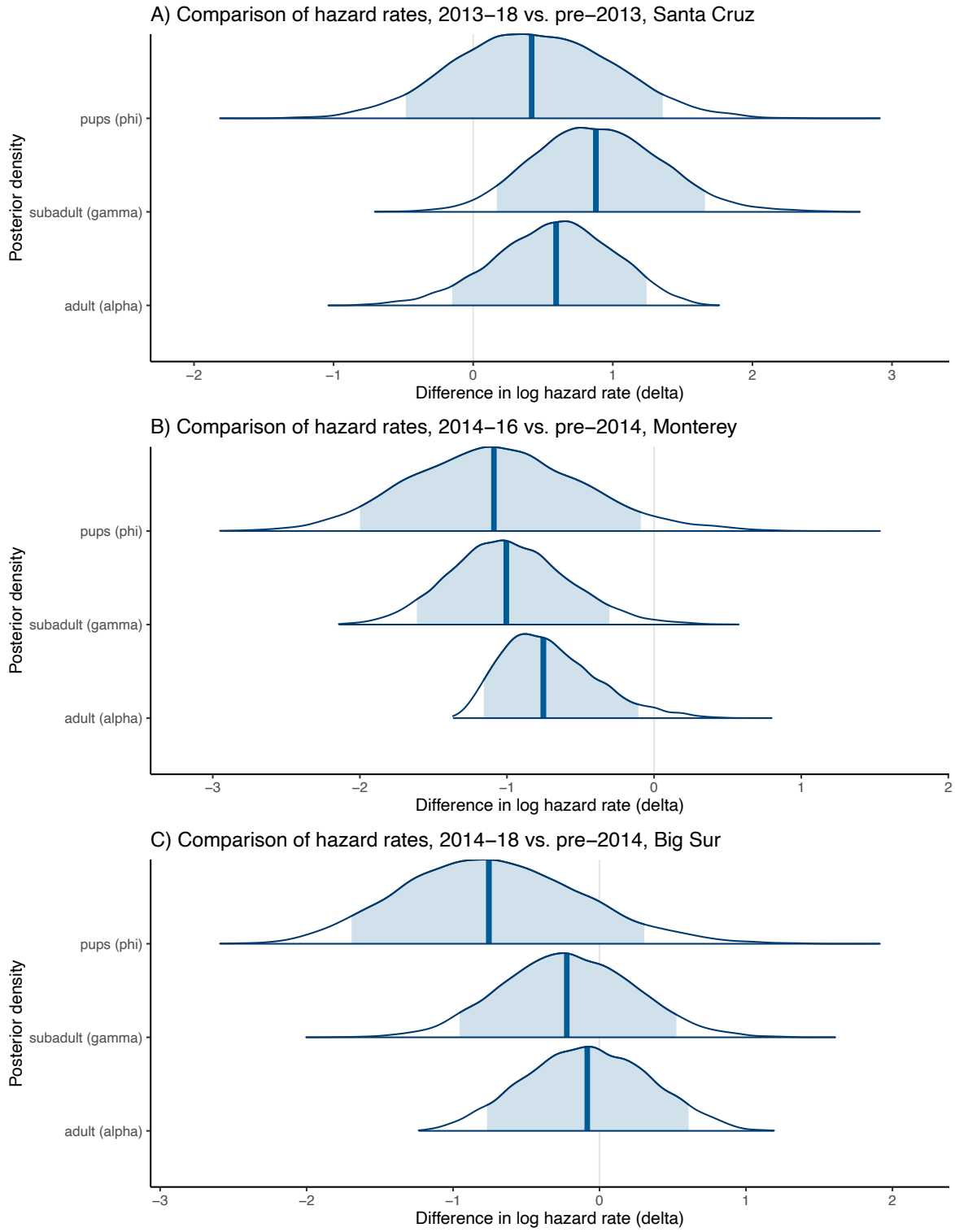

Figure S5. Trends in total abundance of sea otters for Santa Cruz (green line), Monterey (orange line), and Big Sur (blue line) as estimated by a Bayesian state space model. Each shaded band represents the 95% credible intervals (CI) around the mean estimated values.

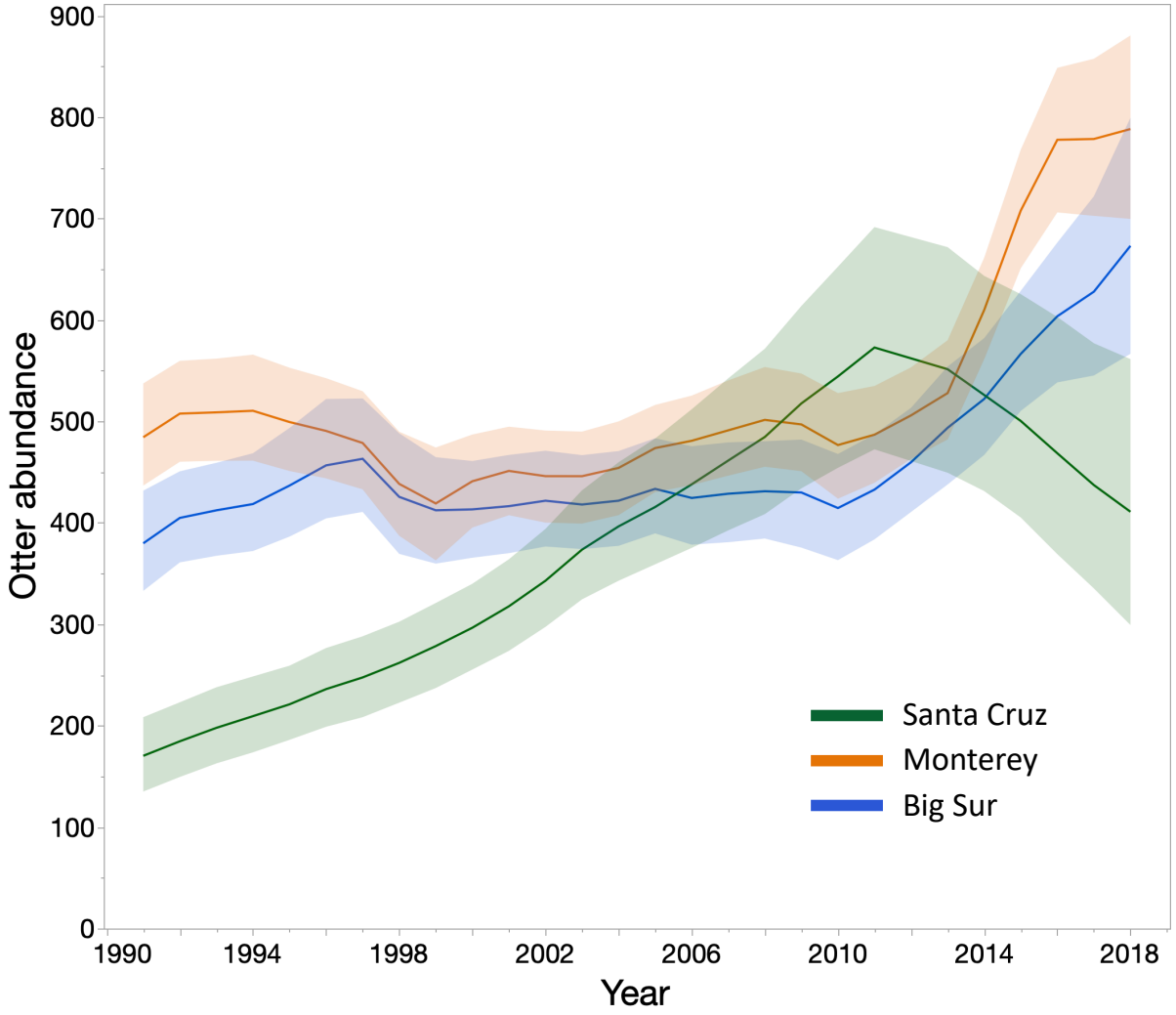

Figure S6. Dietary mean proportion of sea urchins for sea otters specializing on individual prey items before (2000-2013) and after (2014-2018) the urchin outbreak. Error bars are 95% confidence intervals surrounding the mean.

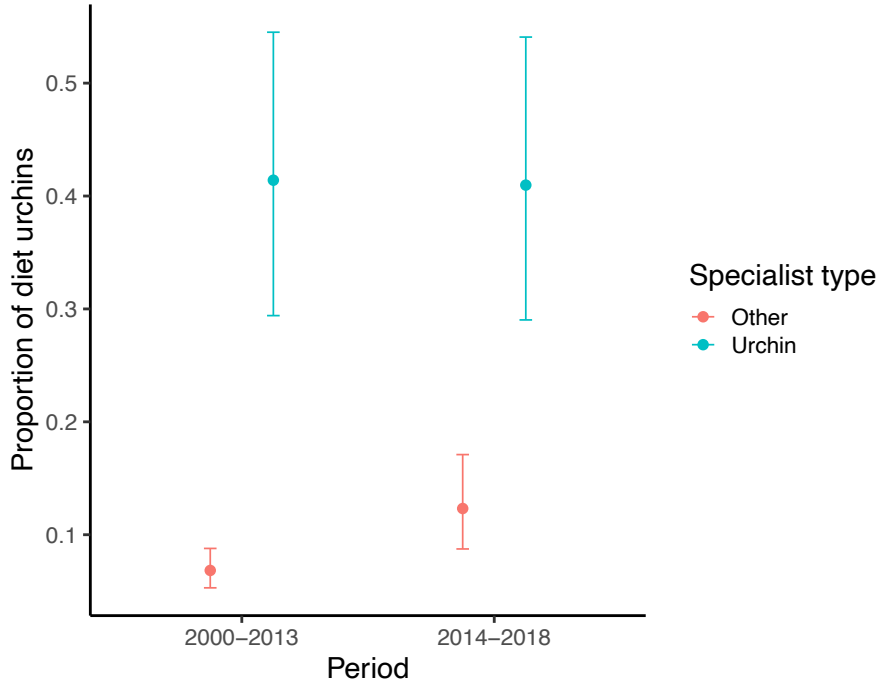

Figure S7. Population-level dietary mean proportion of sea urchins in sea otter diets before (2000-2013) and after (2014-2018) the urchin outbreak. Error bars are 95% confidence intervals surrounding the mean.

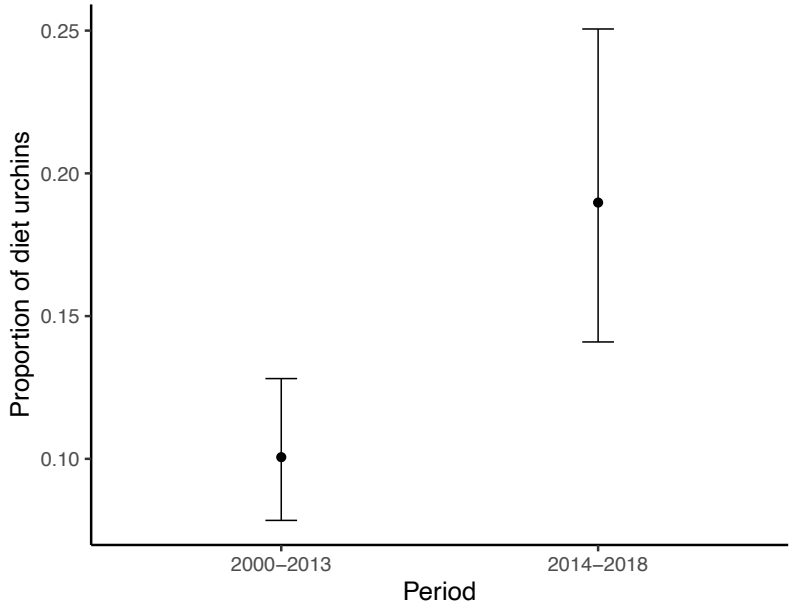

Figure S8. Estimated proportional contributions to southern sea otter diets of urchins, mussels, and urchins and mussels combined, based on observational data collected in the Monterey study area during two time periods: 2000-2013, and 2014-2018. Relative dietary abundance is measured in terms of the proportion of total consumed biomass contributed by each prey type, based on fitting a Monte Carlo-based re-sampling model to observational field data collected from foraging otters (15), and incorporating the empirically derived functional relationships between prey diameter (estimated by observers via comparison with known paw widths) and edible biomass.

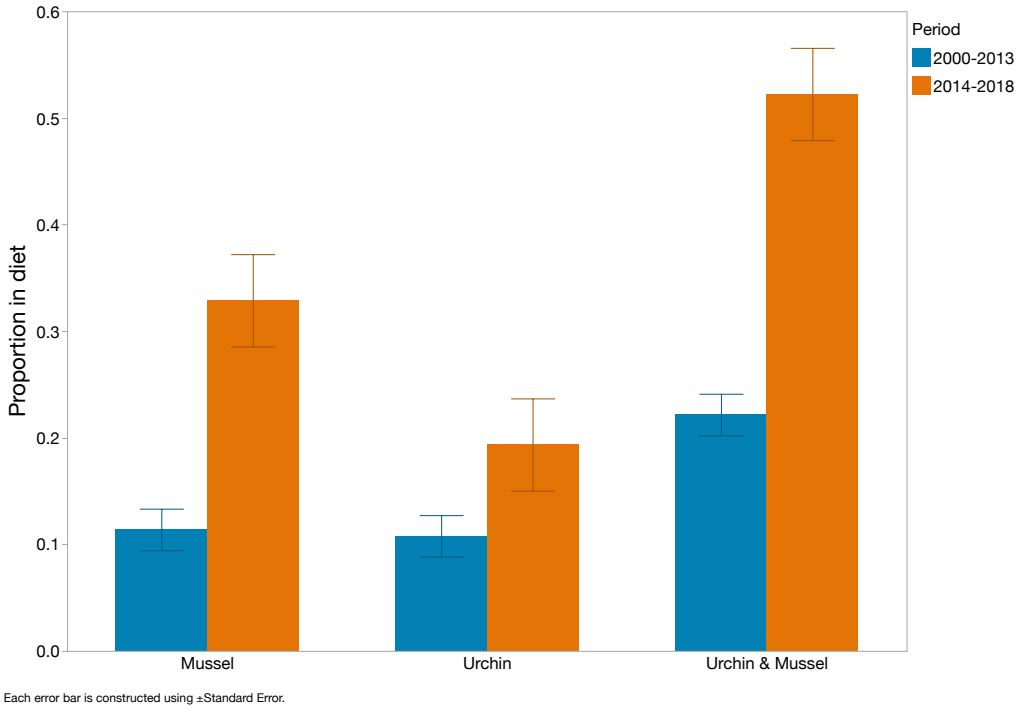

Figure S9. Subtidal radial sampling design. Each line radiating from the center of the site represents a 5-meter long transect with two 1-m^2 quadrats (16 quadrats per site). Quadrats were randomly stratified in order to avoid over or under-sampling by accounting for increasing arc length with increasing distance from the center of the site. The radial sampling design was selected in order to compliment shore observations of sea otter foraging, where a sub-bout was recorded at the surface as any number of repetitive dives made within a 10-meter diameter zone.

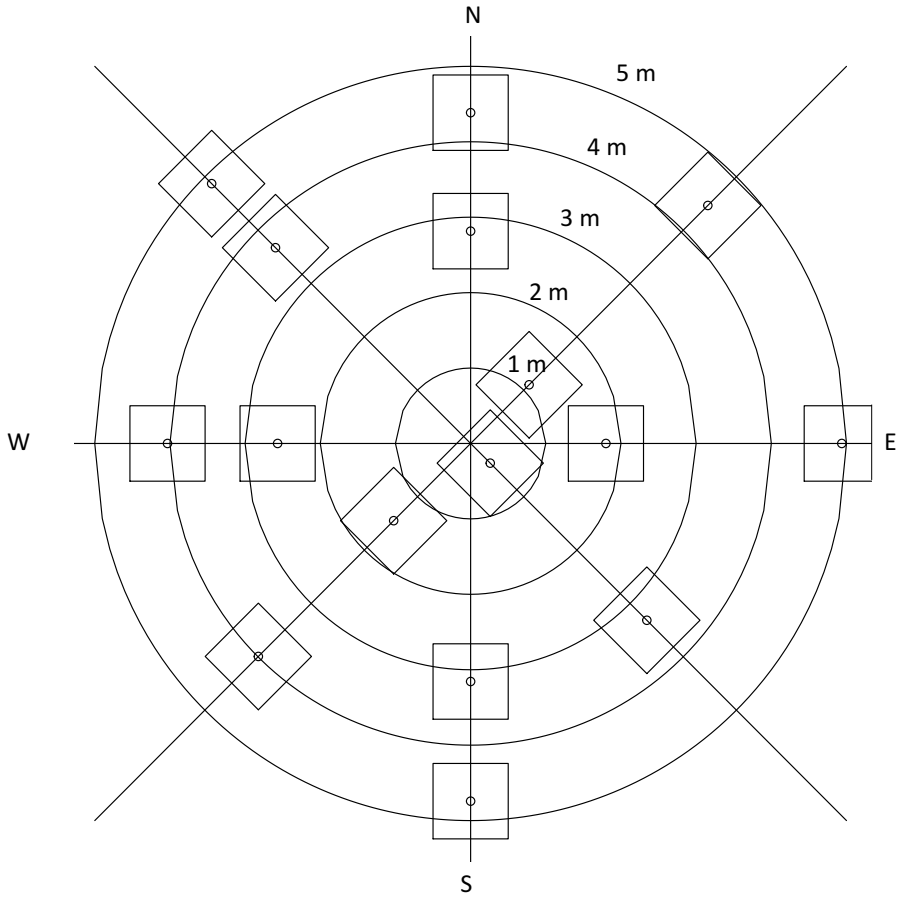

Figure S10. Sea otter population survey regions along the central coast of California, USA.

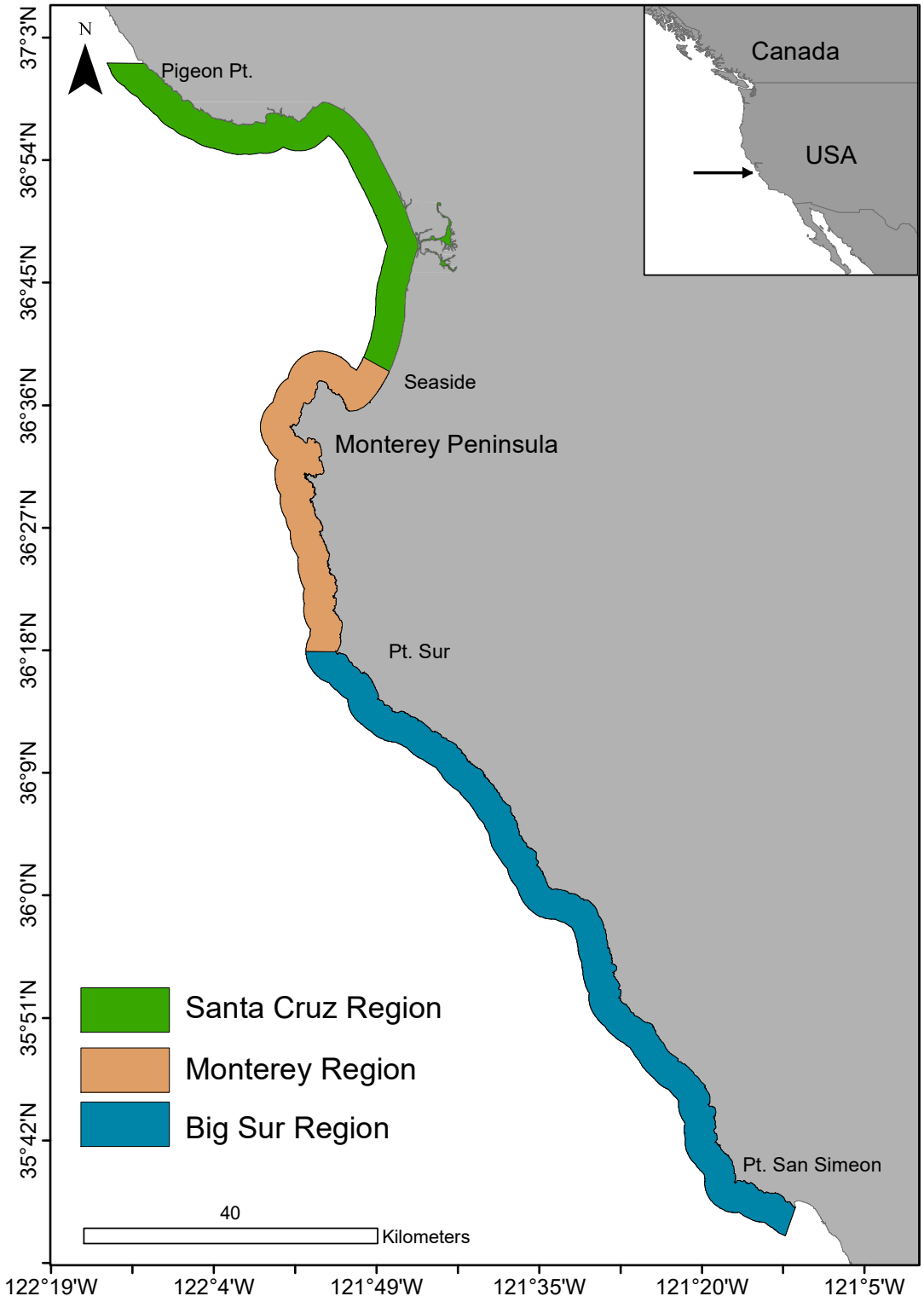

Figure S11. Relative kelp stipe density (A), proportion of exposed (i.e., active foraging) urchins (B), mean urchin density (C), and mean gonad index (D) between reference survey sites (green) and sea otter focal patches (orange) with 95% confidence intervals surrounding each mean.

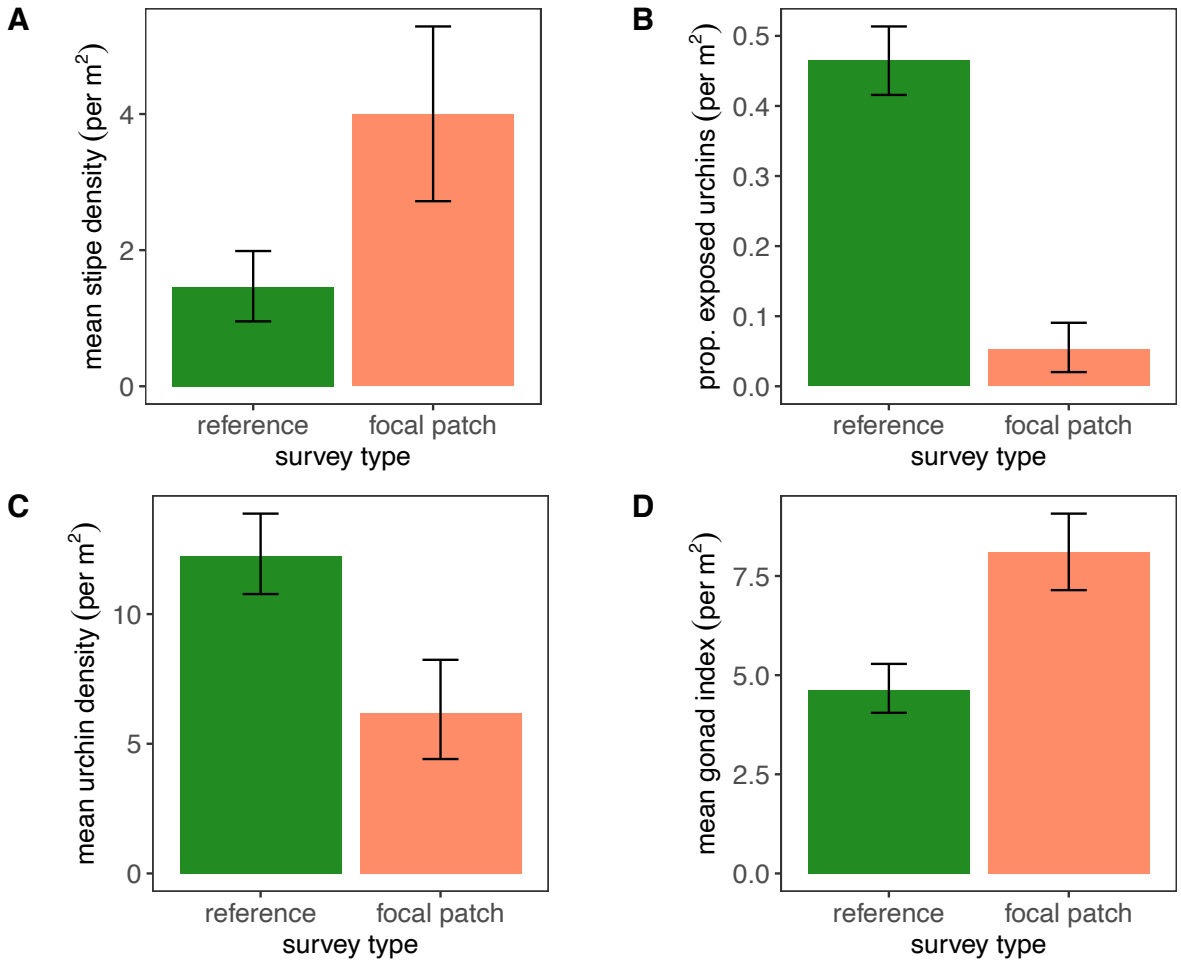

Figure S12. Posterior predictive check plots for a Bayesian state-space model fit to sea otter survey data from the Monterey region. Panel A) shows the mean observed value of independent otters from all surveys (vertical black line) compared to a frequency distribution of out-of-sample predictions from the model (the observed value should be in the center of the distribution for a well-fit model). Panel B) shows a density plot of observed counts across years, with grey lines showing replicate density plots for out-of-sample predictions.

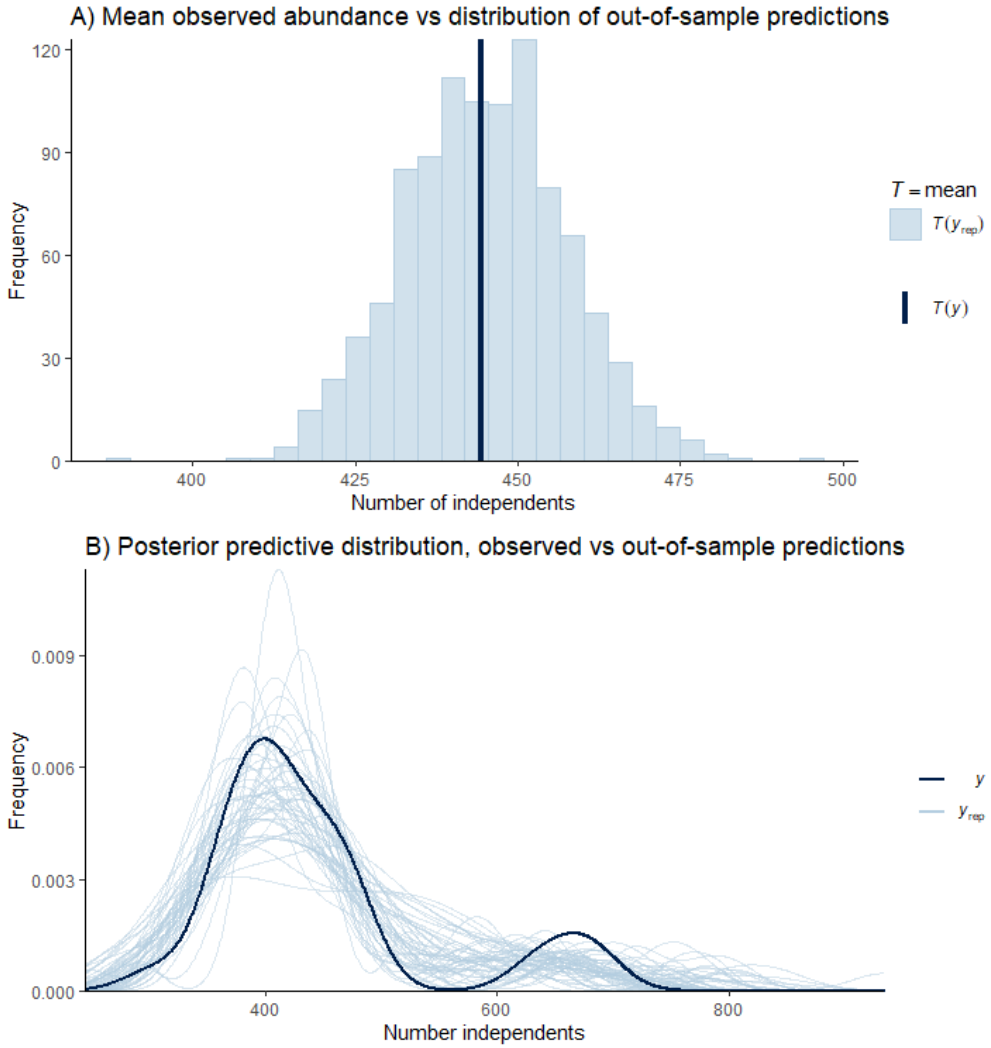

References

1. B. B. Hatfield, J. L. Yee, M. C. Kenner, J.A. Tomoleoni, M. T. Tinker, Annual California sea otter census–2018 spring census summary. U.S. Geological Survey data release (2018a). https://doi.org/10.5066/P98012HE

2. B. B. Hatfield, J. L. Yee, M. C. Kenner, J. A. Tomoleoni, M. T. Tinker, California sea otter (Enhydra lutris nereis) census results, spring 2018. U.S. Geological Survey Report 1097, Reston, VA (2018).

3. M. T. Tinker, *et al.*, Incorporating diverse data and realistic complexity into demographic estimation procedures for sea otters. *Ecol. Appl.* **16**, 2293–2312 (2006).

4. M. T. Tinker, *et al.,* Trends and Carrying Capacity of Sea Otters in Southeast Alaska. Journal of Wildlife Management **early edition** (2019).

5. L. L. Eberhardt, Using the Lotka-Leslie Model for Sea Otters Author. *Wildl. Soc.* **59**, 222–227 (2019).

6. L. R. Gerber, M. T. Tinker, D. F. Doak, J. A. Estes, D. A. Jessup, Mortality sensitivity in life-stage simulation analysis: a case study of southern sea otters. *Ecol. Appl.* **14**, 1554-1565 (2004).

7. M. T. Tinker, *et al,* Southern sea otter range expansion and habitat use in the Santa Barbara Channel, California. US Geological Survey Open File Report **2017-1001**:76p (2017).

8. M. L. Riedman, J. A. Estes, M. M. Staedler, A. A. Giles, D. R. Carlson, Breeding patterns and reproductive success of California sea otters. *J. Wildl. Manage.* **58**, 391 (1994).

9. R. J. Jameson, A. M. Johnson, Reproductive Characteristics of Female Sea Otters. *Mar. Mammal Sci.* **9**, 156–167 (1993).

10. M. T. Tinker, *et al.,* Southern sea otter (Enhydra lutris nereis) population biology at Big Sur and Monterey, California – Investigating the consequences of resource abundance and anthropogenic stressors for sea otter recovery. U.S. Geological Survey Report 2019-1022, Reston, VA (2019).

11. B. Carpenter, *et al.*, Stan: A probabilistic programming language. *J. Stat. Softw.* **76** (2017).

12. A. Gelman, J. B. Carlin, H. S. Stern, D. B. Rubin, Bayesian Data Analysis. *J. Am. Stat. Assoc.* **109**, 1325–1337 (2014).

13. A. Gelman, Y. Goegebeur, F. Tuerlinckx, I. Van Mechelen, Diagnostic checks for discrete data regression models using posterior predictive simulations. *J. R. Stat. Soc. Ser. C Appl. Stat.* **49**, 247–268 (2000).

14. A. Vehtari, A. Gelman, J. Gabry, Practical Bayesian model evaluation using leave-one-out cross-validation and WAIC. *Stat. Comput.* **27**, 1413–1432 (2017).

15. M. Tim Tinker, *et al.*, Structure and mechanism of diet specialisation: Testing models of individual variation in resource use with sea otters. *Ecology* **15**, 475–483 (2012).